

COMPUTATION OF TSUNAMI AMPLITUDES RESULTING FROM A PREDICTED MAJOR EARTHQUAKE IN THE SHUMAGIN SEISMIC GAP

Zygmunt Kowalik

Institute of Marine Science, University of Alaska

T. S. Murty

Institute of Ocean Sciences, Department of Fisheries and Oceans

Abstract. A time-dependent two-dimensional numerical model was developed to study the generation and propagation of a tsunami resulting from a major earthquake predicted to occur in the Shumagin Seismic Gap area of the eastern part of the Aleutian Island chain. The grid size is approximately 28 km in the latitudinal direction and 36 km in the longitudinal direction. The leading wave of the tsunami took only about three hours to arrive at the southern British Columbia coast and the northern part of the coast of the state of Washington. On the other hand, it took about eight hours to propagate into the Bering Sea. Two important results emerged from this study. The tsunami waves show very strong directionality, and the presence of the so-called lateral waves can be inferred. In the deep ocean, tsunami amplitudes up to one meter appear to occur. To deduce the detailed distribution of the tsunami amplitudes at the coast, the present large area model has to be coupled to a coastal model which uses either finer rectangular grids or irregular triangular grids.

Introduction

Three major seismic gaps—Yakataga, Shumagin and Unalaska (Figure 1) have been identified by Sykes [1971] and Kelleher et al. [1973] along the southern coastal belt of Alaska-Aleutian region. However, due to a lack of reliable historical earthquake data for this region, the available estimates of repeat time varies widely in the range of 60 to 1000 years. On the basis of an average value of 6 cm/year for the plate motion, a repeat time of 200 years has been estimated by Kanamori [1977] for the above region.

Despite a general uncertainty in the estimation of repeat times as mentioned above, an examination of the available earthquake catalog for Alaska [Cox et al., 1976] shows that three strong earthquakes (in the years 1788, 1847 and 1903) have occurred within the area identified as the Shumagin Gap. Sykes [1971], Kelleher et al. [1973], Davies et al. [1981] and Beavan et al. [1983] therefore suggested the possibility of occurrence of a major earthquake within the Shumagin Gap in the next two decades. It is expected that the moment magnitude M_w of the earthquake will be about 8.4. The most recent paper on this topic is by Jacob [1984] in which a high probability is given to the occurrence of a major earthquake in the Shumagin Gap.

Although the direct effects of such an earthquake will be con-

finied to the Aleutians and some parts of Alaska, there is no doubt that an earthquake of this magnitude (about the same as the Alaska earthquake of March 28, 1964) will generate a major tsunami that will travel across the Pacific Ocean to various coastlines. Our aim here is to simulate the tsunami waves that might result from this predicted large earthquake. This will be done in two stages. In the first stage we simulate the generation of the tsunami and its propagation in the deep ocean. These calculations can be performed on a relatively coarse grid such as that shown in Figure 2. These deep water signatures [Murty, 1977; Saxena, 1983; Zielinski and Saxena, 1983] will provide boundary conditions for a coastal model which uses a finer grid. Here we report the results from the first phase of the study, the work on the second phase is in progress at present.

We believe that the amplitudes of the tsunami waves shown below are accurate for the deep water and are under-estimates for the coastal region. Later computations with a finer grid for the coast will most probably give values of tsunami amplitudes somewhat greater than shown here for the coast. Traditionally for impulsive earthquakes (i.e., earthquakes in which the bottom motion is completed within a few seconds), the initial water surface wave amplitude is taken equal to the vertical amplitude of the bottom motion [Murty, 1977]. The tsunami travel times computed here are believed to be accurate.

The Numerical Model

The equations of motion and continuity in a spherical polar coordinate system are [e.g., see Murty, 1984]

$$\frac{\partial U}{\partial t} - rV + \frac{KU}{H} + \frac{g}{R \cos \phi} \frac{\partial \eta}{\partial \lambda} = 0 \tag{1}$$



Fig. 1. Seismic gaps in the Alaska-Aleutians area.

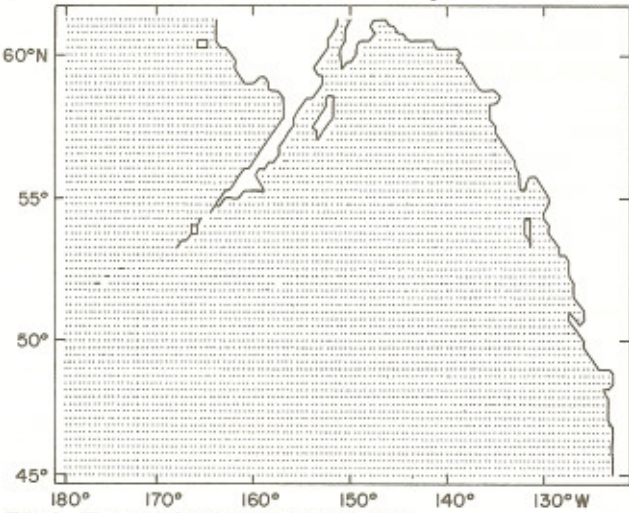


Fig. 2. The grid for the numerical model.

$$\frac{\partial V}{\partial t} + fU + \frac{KV}{H} + \frac{g}{R} \frac{\partial \eta}{\partial \phi} = 0 \quad (2)$$

$$\frac{1}{R \cos \phi} \frac{\partial}{\partial \lambda} (HU) + \frac{\partial}{\partial \phi} (HV \cos \phi) + \frac{\partial \eta}{\partial t} = 0 \quad (3)$$

Here λ is the east longitude, ϕ is the north latitude, R is the radius of the earth, f is the coriolis parameter, g is gravity, $H(\lambda, \phi)$ is the water depth in the equilibrium state and η is the deviation of the free surface from the equilibrium level; here U and V are the east and north components of the depth-averaged currents, t is time and K is a linear bottom friction coefficient.

In this deep ocean model, we have not included the nonlinear advective terms and the horizontal frictional terms, since these terms are expected to make no significant contribution. As for the boundary conditions, a radiation condition was used at the open boundaries and at the shore the normal velocity is equated to zero. The grid scheme and the finite-difference forms used here are similar to those in Ramming and Kowalik [1980]. The

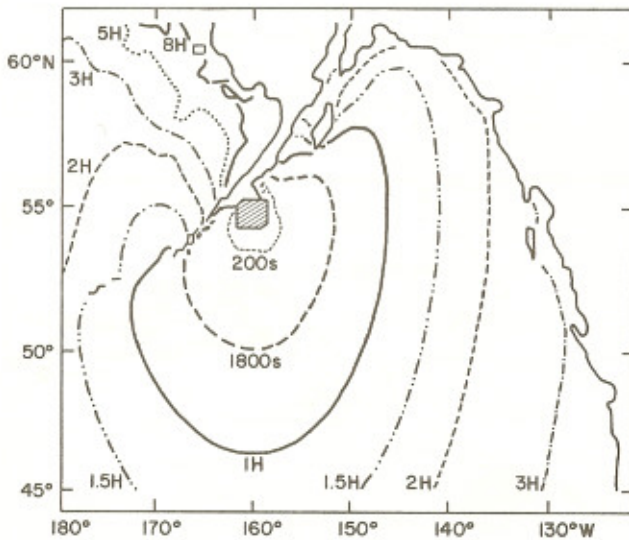


Fig. 3. Tsunami travel-time contours. The dark area shows the source region.

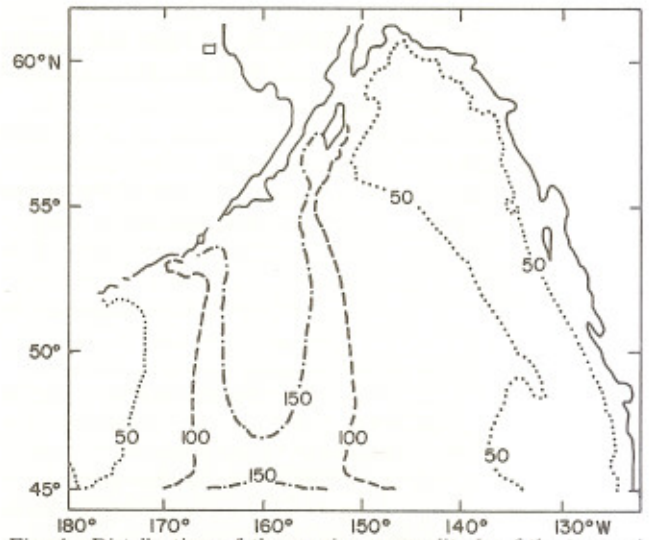


Fig. 4. Distribution of the maximum amplitude of the tsunami (cm).

model is calibrated against tides and storm surges in the polar regions [Kowalik and Matthews, 1982]. Since tsunamis are long gravity waves such as tides and storm surges, the model calibration is believed to be valid for tsunamis also.

Discussion of Results

Figure 3 shows the travel time curves. The hatched area is the earthquake source. A vertical displacement of 10 m was assumed for the bottom motion, somewhat similar to the Alaska earthquake of March 1964. It can be seen that the tsunami travelled

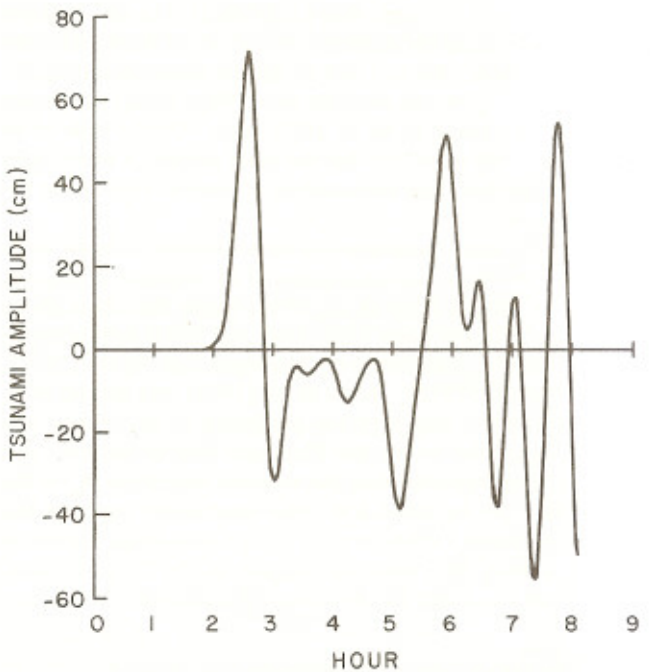


Fig. 5. Computed tsunami amplitudes (cm) as a function of time at Seward, Alaska. Zero time refers to the instant of tsunami generation.

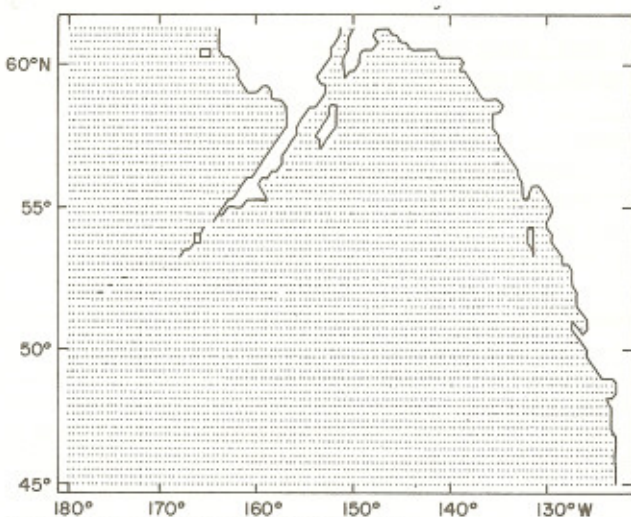


Fig. 2. The grid for the numerical model.

$$\frac{\partial V}{\partial t} + fU + \frac{KV}{H} + \frac{g}{R} \frac{\partial \eta}{\partial \phi} = 0 \quad (2)$$

$$\frac{1}{R \cos \phi} \frac{\partial}{\partial \lambda} (HU) + \frac{\partial}{\partial \phi} (HV \cos \phi) + \frac{\partial \eta}{\partial t} = 0 \quad (3)$$

Here λ is the east longitude, ϕ is the north latitude, R is the radius of the earth, f is the coriolis parameter, g is gravity, $H(\lambda, \phi)$ is the water depth in the equilibrium state and η is the deviation of the free surface from the equilibrium level; here U and V are the east and north components of the depth-averaged currents, t is time and K is a linear bottom friction coefficient.

In this deep ocean model, we have not included the nonlinear advective terms and the horizontal frictional terms, since these terms are expected to make no significant contribution. As for the boundary conditions, a radiation condition was used at the open boundaries and at the shore the normal velocity is equated to zero. The grid scheme and the finite-difference forms used here are similar to those in Ramming and Kowalik [1980]. The

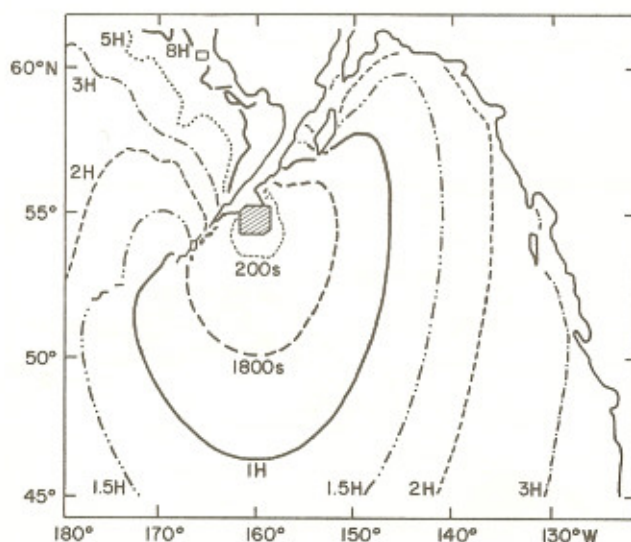


Fig. 3. Tsunami travel-time contours. The dark area shows the source region.

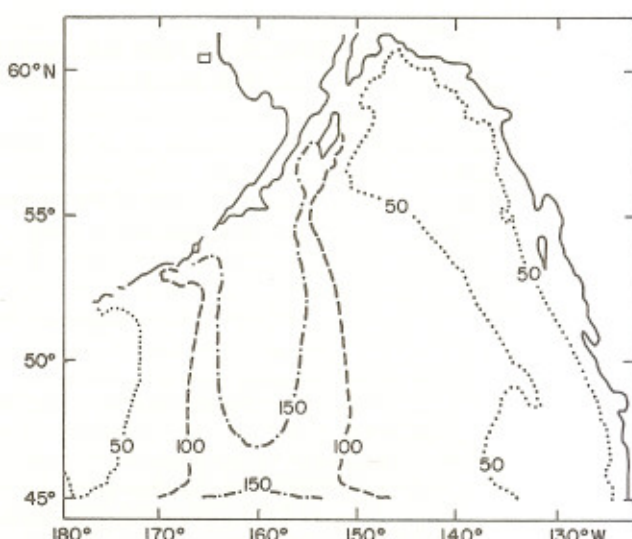


Fig. 4. Distribution of the maximum amplitude of the tsunami (cm).

model is calibrated against tides and storm surges in the polar regions [Kowalik and Matthews, 1982]. Since tsunamis are long gravity waves such as tides and storm surges, the model calibration is believed to be valid for tsunamis also.

Discussion of Results

Figure 3 shows the travel time curves. The hatched area is the earthquake source. A vertical displacement of 10 m was assumed for the bottom motion, somewhat similar to the Alaska earthquake of March 1964. It can be seen that the tsunami travelled

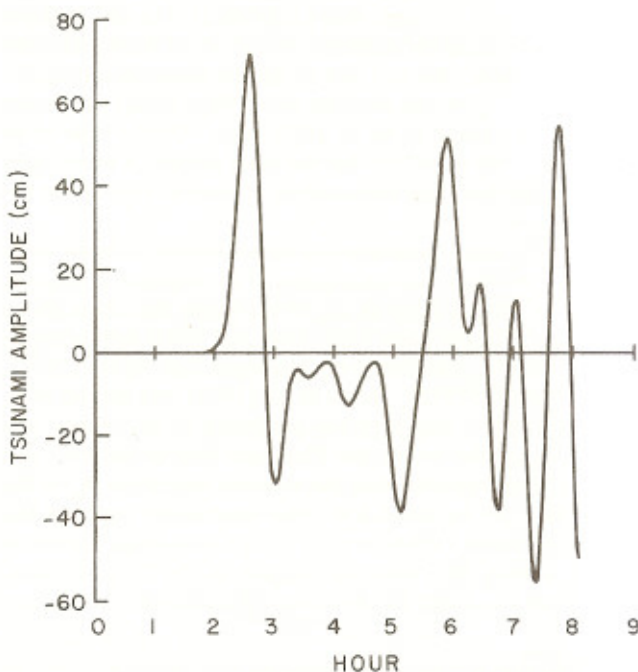


Fig. 5. Computed tsunami amplitudes (cm) as a function of time at Seward, Alaska. Zero time refers to the instant of tsunami generation.

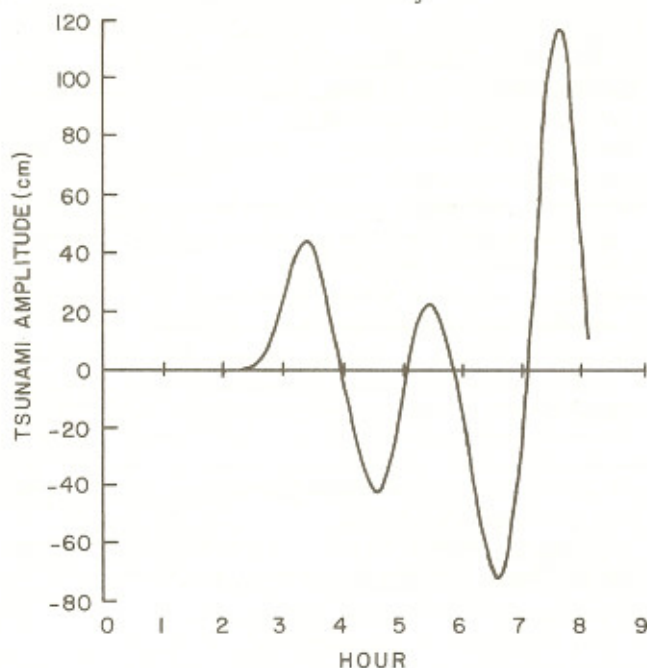


Fig. 6. Computed tsunami amplitudes as a function of time at Valdez, Alaska.

fastest in the deep ocean towards south, southwest and southeast. Whereas it only took about three hours for the tsunami to arrive near the coast of the State of Washington, it took about five hours to penetrate into Cook Inlet and more than eight hours to propagate into the shallow Bering Sea.

To study the directional properties of tsunami amplitude distribution, at each grid point, the amplitudes were compared throughout the duration of the computation and the highest

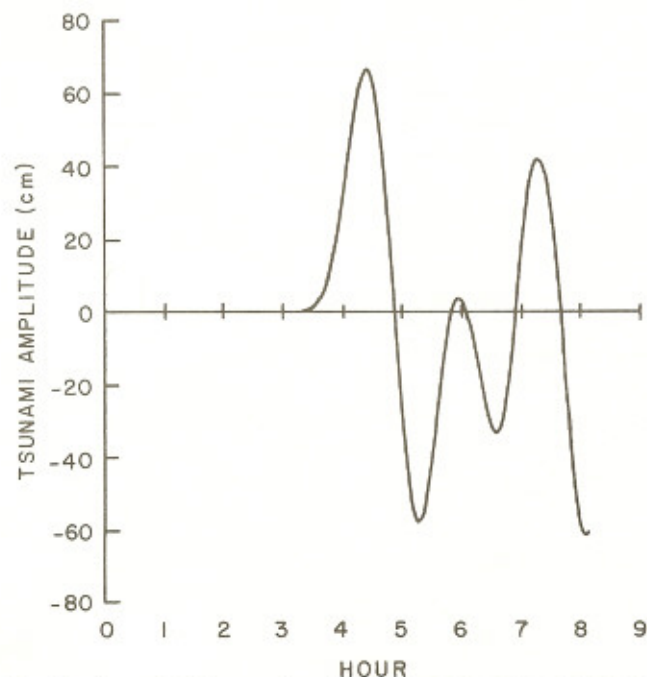


Fig. 7. Computed tsunami amplitudes as a function of time at Prince Rupert, British Columbia, Canada.

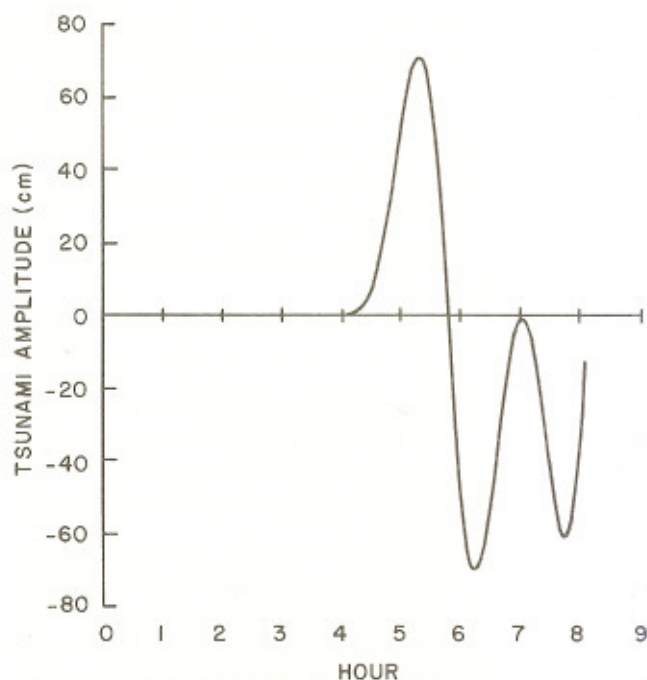


Fig. 8. Computed tsunami amplitudes as a function of time at the mouth of the Juan de Fuca Strait.

amplitude was tabulated. The distribution of this amplitude, which we shall call a maximum amplitude, is plotted in Figure 4. It can be seen that the greatest values of the maximum amplitude of up to 1.5 m in the deep ocean occur in a zone directly south of the Shumagin Gap and are centered on the 160°W longitude. Note that the 160°W longitude also intersects the Hawaiian Islands. Thus one of the important results of this study is that the tsunami energy shows strong directionality; the tsunami not only travels faster towards Hawaii, but a substantial portion of the tsunami energy may be radiated in that direction. Another result is that the effects of the so-called lateral waves [Murty and Loomis, 1983] can be seen in the Gulf of Alaska-Cook Inlet area.

Figures 5 to 8 respectively show the computed tsunami amplitudes at Seward, Valdez, Prince Rupert (British Columbia) and mouth of the Juan de Fuca Strait. As pointed out above, these amplitudes might be somewhat under-estimated by the crude grid model. In any case, the tsunami ranges shown here (for example, the range at Valdez is about 2.10 m) are quite significant and are capable of causing destruction, especially if the peak tsunami (largest wave) arrives at the time of high tide.

Acknowledgments. We thank Coralie Wallace for drafting the diagrams.

This is Contribution No. 567, Institute of Marine Science, University of Alaska, Fairbanks, Alaska 99701.

References

- Beavan, J., E. Hauksson, S. R. McNutt, R. Bilham and K. H. Jacob, Tilt and seismicity changes in the Shumagin seismic gap, *Science*, 222, 322, 1983.
- Bilham, R., Tsunami-resistant gauges for epicentral sea-level studies, *Proc. Tsunami Symp.*, Hamburg, edited by E. N. Bernard, 155, Aug. 1983.

- Cox, D. C., G. Fararas-Carayannis and J. P. Calcebaugh, Catalog of Tsunamis in Alaska, World Data Center A for Solid Earth Geophysics, Rept. SE-1, NOAA, Asheville, N.C., 43 pp., 1976.
- Davies, J. N., L. R. Sykes, L. House and K. Jacob, Shumagin seismic gap, Alaska Peninsula: history of great earthquakes, tectonic settings and evidence of high seismic potential, *J. Geophys. Res.*, 86, 3821, 1981.
- Jacob, K. H., Estimates of long-term probabilities for future great earthquakes in the Aleutians, *Geophys. Res. Lett.*, 11, 295-298, 1984.
- Kanamori, H., Seismic and aseismic slip along subduction zones and their tectonic implications, in *Island Arcs and Deep-Sea Trenches and Back-Arc Basins*, edited by M. C. Talwani and W. C. Pitman, (III), A.G.U., Washington, D.C., 1977.
- Kelleher, J., L. R. Sykes and J. Oliver, Possible criteria for predicting earthquake locations and their application to major plate boundaries at the Pacific and Caribbean, *J. Geophys. Res.*, 78, 2547, 1973.
- Kowalik, Z. and J. B. Matthews, The M_2 tide in the Beaufort and Chukchi Seas, *J. Phys. Oceanography*, 12, 7, 743-746, 1982.
- Murty, T. S., Seismic sea waves-tsunamis, Bull. 198, Fisheries Res. Board Canada, Ottawa, 337 pp., 1977.
- Murty, T. S. and H. G. Loomis, Diffracted long waves along continental shelf edges, *Proc. Tsunami Symp.*, Hamburg, edited by E. N. Bernard, 211, Aug. 1983.
- Murty, T. S., *Storm Surges—Meteorological Ocean Tides*. Bull. 212, Fisheries Res. Board Canada, Ottawa, 897 pp., 1984.
- Ramming, H. G. and Z. Kowalik, *Numerical Modelling of Marine Hydrodynamics*, Elsevier, 368 pp., 1980.
- Saxena, N. K., Marine geodetic applications for ocean sciences and engineering, *Marine Geodesy*, 7, 39, 1983.
- Sykes, L. R., Aftershock zones of great earthquakes, seismicity gaps, earthquake prediction for Alaska and the Aleutians, *J. Geophys. Res.*, 76, 8021, 1971.
- Zielinski, A. and N. K. Saxena, Rationale for measurement of midocean tsunami signature, *Marine Geodesy*, 6, 331, 1983.
- Zielinski, A. and N. K. Saxena, Tsunami detectability using open-ocean bottom pressure fluctuations, *I.E.E.E.J. Oceanic Eng.*, OE-8, 272, 1983.

Z. Kowalik, Institute of Marine Science, University of Alaska, Fairbanks, Alaska 99701, USA.

T. S. Murty, Institute of Ocean Sciences, Department of Fisheries and Oceans, P.O. Box 6000, Sidney, B.C., Canada V8L4B2.

(Received September 7, 1984;
accepted October 2, 1984.)